NUMERICAL STUDY OF THE FLEXURAL BEHAVIOUR OF GFRP RC BEAMS

Dawid PAWŁOWSKI [a*], Maciej SZUMIGAŁA [b]

[a] PhD Student; Faculty of Civil and Environmental Engineering, Poznań University of Technology, Piotrowo 5, 60-965 Poznań
E-mail address: *dawid.p.pawlowski@doctorate.put.poznan.pl*

[b] Associate Prof.; Faculty of Civil and Environmental Engineering, Poznan University of Technology, Piotrowo 5, 60-965 Poznań, Poland

Received: 15.10.2014; Revised: 15.10.2014; Accepted: 28.01.2015

Abstract
Fiber-reinforced polymer (FRP) bars have been commercially available in civil engineering in the last twenty years. Due to their mechanical and physical properties, the behaviour of FRP reinforced concrete (RC) members is significantly different to that of traditional steel RC. This paper presents the results and discussion of a numerical study of the flexural behaviour of simply supported glass fiber-reinforced polymer (GFRP) RC beams under short-term static loads. The numerical analysis was performed using the Finite Element Method (FEM). All calculations were carried out in the environment of the Abaqus. The main objective of this paper was to investigate the flexural behaviour of GFRP RC members depending on the reinforcement ratio. The results of the numerical analysis were examined and compared with code formulations and with the results of experiments.

Streszczenie
Zbrojenie kompozytowe (FRP) jest wykorzystywane w budownictwie od ponad dwudziestu lat. Ze względu na jego mechaniczne i fizyczne właściwości, zachowanie elementów zbrojonych prętami niemetalicznymi jest odmienne od zachowania klasycznych elementów żelbetowych. W pracy przedstawiono wyniki symulacji komputerowej zachowania swobodnie podpartych belek zbrojonych prętami z włókna szklanego (GFRP) poddanych działaniu krótkotrwałego obciążenia statycznego. Badanie numeryczne przeprowadzono przy zastosowaniu oprogramowania Abaqus wykorzystującego Metodę Elementów Skończonych (MES).
Głównym celem pracy było zbadanie wpływu stopnia zbrojenia na nośność i sztywność elementów zbrojonych prętami GFRP. Wyniki symulacji komputerowej porównano z wynikami normowymi oraz z rezultatami doświadczeń laboratoryjnych.

Keywords: **Composite materials; GFRP reinforcement; GFRP RC beams; Flexural behaviour; FEM analysis.**

1. INTRODUCTION

Fiber-reinforced polymer (FRP) bars have emerged as an alternative reinforcement for concrete structures. On the one hand, this kind of reinforcement exhibits such properties as corrosion resistance, electromagnetic neutrality and high cuttability [1]. As a result it can have many applications, especially in structures used in marine environments, in chemical plants, when electromagnetic neutrality is needed, or in temporary structures.

On the other hand, FRP bars have low modulus of elasticity and high tensile strength [2]. Due to their mechanical properties, deflections and cracking of FRP RC flexural members are larger than of traditional RC members. As a result, the design of FRP RC beams is often governed by the serviceability limit states [3].

This paper presents the results of a numerical study in which three GFRP RC beams were tested in four-point bending. The aim of this simulation was to examine the failure mechanism and deflections of sim-

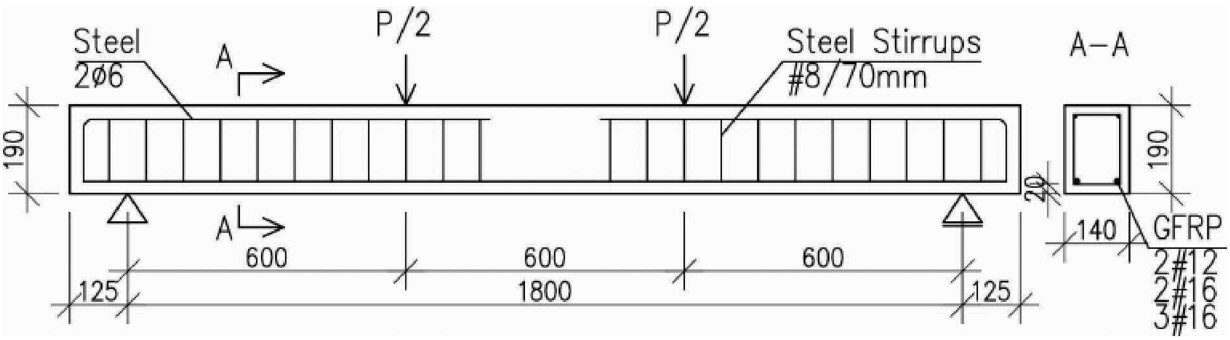

Figure 1.
Geometry and reinforcement of specimen [mm]

ply supported GFRP RC beams depending on the reinforcement ratio. The dimensions of the specimens and properties of concrete and GFRP bars were assumed on the basis of an experimental study [4]. The results of the numerical simulation were compared with code formulations [2, 5] and with the results of experimental tests [4].

2. NUMERICAL SIMULATION

2.1. Test specimens

The numerical model of beams was created on the basis of the beam which is shown in Fig. 1.

The numerical study consisted in investigating the flexural behaviour of three beams with varying GFRP reinforcement (Tab. 1). All beams had a cross-section of 0.14×0.19 m^2, a total length of 2.05 m and a span of 1.80 m. The shear reinforcement consisted of 8 mm round steel stirrups placed at intervals of 70 mm. In the pure bending zone no stirrups were provided. Two 6 mm steel bars were used as top reinforcement to hold the stirrups.

Table 1.
Characteristics of specimens

Beam designation	Main bar	Reinforcement ratio ρ_f [%]
…-2#12	2#12	0.99
…-2#16	2#16	1.77
…-3#16	3#16	2.66

2.2. Materials properties

Concrete

All beams had a target concrete compressive strength of 30 MPa. The properties of concrete were evaluated from cylindrical specimens. They are presented in Tab. 2.

Table 2.
Mechanical properties of concrete

Modulus of elasticity E_c [GPa]	Compressive strength f_c [MPa]	Tensile strength f_{ct} [MPa]
25.8	32.1	2.8

GFRP

GFRP ribbed bars were used as a flexural reinforcement. The experimentally determined mechanical properties of reinforcement are shown in Tab 3.

Table 3.
Mechanical properties of GFRP reinforcement

Diameter [mm]	Tensile strength f_{fu} [MPa]	Modulus of elasticity E_f [GPa]
12	1321	63.4
16	1015	64.6

2.3. Model of the beam

The finite element (FE) model of considered beams was implemented in ABAQUS environment [6]. The analysis was performed on 2D model and the following assumptions were adopted:

- Concrete damage plasticity (CDP) model of concrete [7] was assumed,
- Tension stiffening effect was taken into account,
- GFRP reinforcement was assumed as a linear elastic isotropic material,
- Steel reinforcement was assumed as a linear elastic-plastic material with isotropic hardening,
- The reinforcement was modelled as 2-node truss elements embedded in 4-node elements of plane stress (Fig. 2).

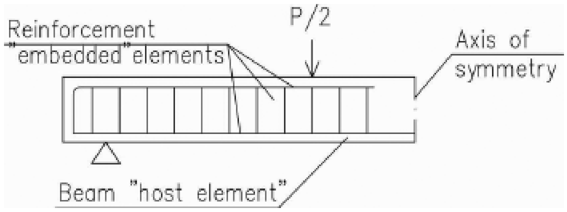

Figure 2.
Scheme of the 2D FE model

The model of beams consisted of two different types of finite element:

- T2D2 – 2-node 2D truss elements,
- CPS4R – 4-node plane stress elements with reduced integration.

The concrete was modelled as concrete damage plasticity material, which is based on the brittle-plastic degradation model [8]. For concrete under uniaxial compression, the stress-strain curve shown in Fig. 3 was adopted. It is composed of the Eurocode 2 [5] parabolic ascending branch and a descending branch extended up to the ultimate strain ε_{cu} [9].

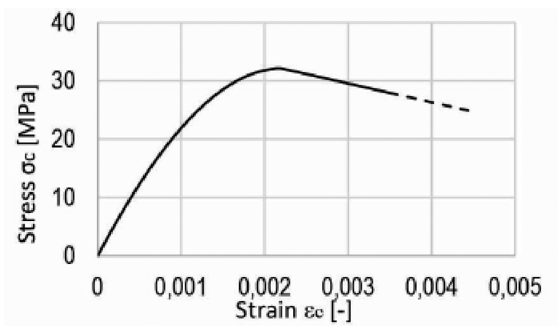

Figure 3.
Response of concrete to uniaxial loading in compression

The tension stiffening effect was taken into account by applying a modified Wang&Hsu [10] formula (Eq. 1) to describe the behaviour of concrete under tension (Fig. 4):

$$\left.\begin{aligned} \sigma_t &= E_c \varepsilon_t, \varepsilon_t \le \varepsilon_{cr} \\ \sigma_t &= f_{ctm}\left(\frac{\varepsilon_{cr}}{\varepsilon_t}\right)^n, \varepsilon_t > \varepsilon_{cr} \end{aligned}\right\} \tag{1}$$

where E_c is the modulus of elasticity of concrete, ε_t is the tensile strain of concrete, ε_{cr} is the tensile strain at concrete cracking, f_{ctm} is the average tensile strength of concrete and n is the rate of weakening.

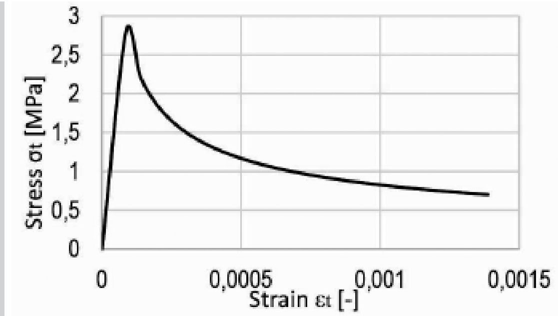

Figure 4.
Response of concrete to uniaxial loading in tension

3. NUMERICAL SIMULATION RESULTS, DATA ANALYSIS AND DISCUSSIONS

3.1. Failure mode and ultimate load

The results of the numerical simulation and the experimental studies [4] shown that all the beams failed in a brittle mode due to concrete crushing. The results of FE analysis are presented in Fig. 5. It was assumed that the value of the maximum compressive concrete strains is about 0.0042.

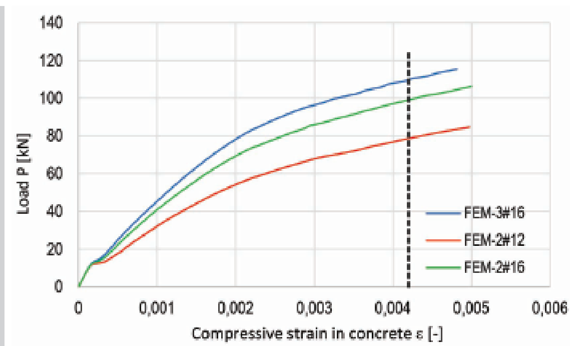

Figure 5.
Ultimate loads (FEM results)

According to ACI 440.1R-06 [2], the failure mode is governed by concrete crushing when the reinforcement ratio ρ_f is greater than the balanced reinforcement ratio ρ_{fb}:

$$\rho_f = \frac{A_f}{bd} \tag{2}$$

$$\rho_{fb} = 0.85\beta_1 \frac{f_c}{f_{fu}} \frac{E_f \varepsilon_{cu}}{E_f \varepsilon_{cu} + f_{fu}} \tag{3}$$

where A_f is the area of GFRP reinforcement, b is the width of the section and d is the effective depth. In Eq. (3), b_1 is the ratio of depth of equivalent rectangular stress block to depth of the neutral axis, f_c is the concrete compressive strength, f_{fu} is the design tensile strength of GFRP reinforcement, E_f is the modulus of elasticity of FRP, and ε_{cu} is the maximum concrete strain (0.003 for ACI 440.1R-06 [2]). The actual and balanced reinforcement ratios are compared in Tab. 4. All the beams had higher reinforcement ratios than ρ_{fb}, hence according to code [2], failure by concrete crushing was expected in all of them. This mode of failure was confirmed by the numerical analysis and the results of experiments [4].

Table 4.
Balanced and actual reinforcement ratio

Beam designation	Actual reinforcement ratio ρ_f [%]	Balanced reinforcement ratio ρ_{bf} [%]
2#12	0.99	0.22
2#16	1.77	0.36
3#16	2.66	0.36

Experimental (EXP), numerical (FEM) and theoretical (ACI for ACI 440.1R-06 and EC2 for Eurocode 2) ultimate loads are compared in Tab. 5. There is good agreement between the experimental and numerical results, whereas ultimate loads calculated according to the codes [2, 5] are underestimated. Their values are lower than the values of loads obtained in the experimental tests [4] by about 26-31% and 10-15% for ACI and EC2, respectively. These differences can be caused by the value of the maximum concrete compressive strain ε_{cu} which is assumed in these codes – 0.0030 for ACI and 0.0035 for EC2. The results of experiments [11] show that the actual ultimate concrete strain ε_{cu} is about 0.0042-0.0047.

On the basis of the results shown in Tab. 5, it can be said that the reinforcement ratio has an influence on the flexural strength of the beams. The increase in the reinforcement ratio results in the increase in the ultimate loads of the beams.

3.2. Deflections

Figs. 6-8 show the numerical, theoretical and experimental load-deflection curves for all beams. The results of the numerical analysis correspond well with the results obtained in the experiments.

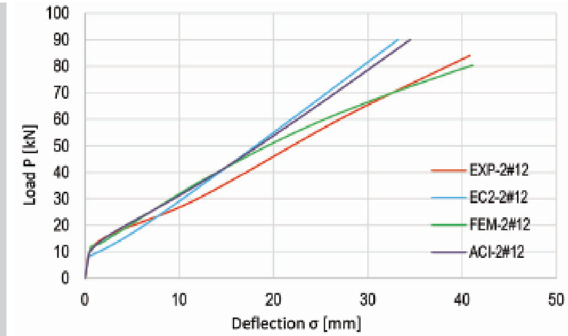

Figure 6.
Experimental, numerical and theoretical load – midspan deflection curves (2#12 beam)

Comparing theoretical predictions obtained based on ACI (Eq. 4) and EC2 (Eq. 5) with the results of experimental tests, it can be observed that up to the service load (deflection d<L/250) there is good agreement between theoretical and actual values of deflections. For higher loads these codes underestimate deflections. These differences can be connected with the fact that these theoretical approaches use a simplified linear stress-strain constitutive relationship for concrete.

$$I_e = \left(\frac{M_{cr}}{M_a}\right)^3 \beta_d I_g + \left[1 - \left(\frac{M_{cr}}{M_a}\right)^3\right] I_{cr} \le I_g \qquad (4)$$

Eq. 4 shows the expression for an effective moment of inertia I_e of the concrete section according to ACI, where I_g is the gross moment of inertia of concrete section, I_{cr} is the moment of inertia of the cracked section, M_{cr} is the cracking moment, M_a is the maximum moment in the member and b_d is the reduction coefficient related to the reduced tension stiffening effect.

Table 5.
Ultimate loads

Beam designation	Reinforcement ratio ρ_f [%]	P_u EXP [kN]	P_u FEM [kN]	P_u ACI [kN]	P_u EC2 [kN]
…2#12	0.99	84	79	64	73
…2#16	1.77	100	99	78	89
…3#16	2.66	112	112	89	102

$$\delta = \zeta \delta_{II} + (1 - \zeta)\delta_I \quad (5)$$

Eq. 5 shows the formulation for deflections d according to Eurocode 2, where d_I is uncracked-state deflection, d_{II} is fully cracked-state deflection and z is the coefficient related to the tension stiffening effect.

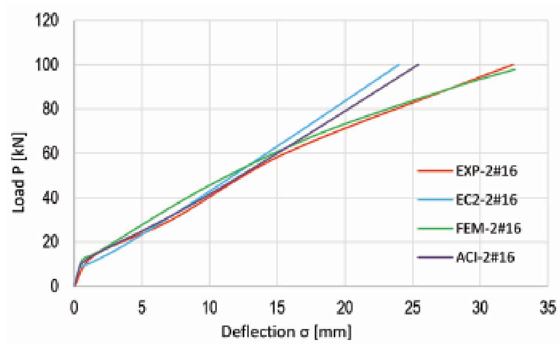

Figure 7.
Experimental, numerical and theoretical load – midspan deflection curves (2#16 beam)

As can be observed in Figs. 6-8, the reinforcement ratio has a significant effect on the stiffness of the RC beams. As expected, higher deflections are obtained for lower reinforcement ratios and vice versa.

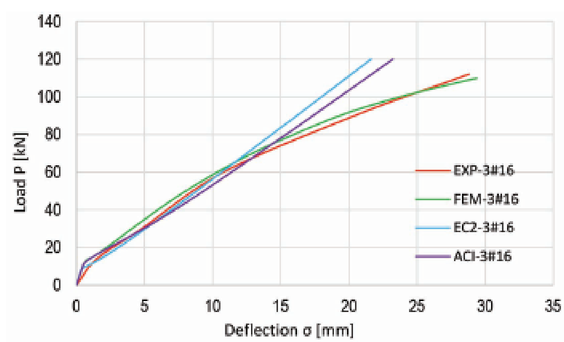

Figure 8.
Experimental, numerical and theoretical load – midspan deflection curves (3#16 beam)

4. CONCLUSIONS

This paper presents the results of numerical, theoretical and experimental study of the flexural behaviour of GFRP RC beams. Based on these results, the following conclusions may be drawn:

- The reinforcement ratio has a significant effect on the flexural behaviour of the GFRP RC beams. The increase in the reinforcement ratio results in the increase in the ultimate loads and in the stiffness of the beams.
- The failure mode is governed by concrete crushing when the reinforcement ratio ρ_f is greater than the balanced reinforcement ratio ρ_{fb} (according to ACI 440.1R-06). All beams behave almost linearly up to the moment of failure, which takes place at relatively large deflections.
- At the service load level, the deflections calculated according to ACI 440.1R-06 and Eurocode 2 are in close agreement with the results of the experiments. For higher loads these codes underestimate deflections.
- The ultimate loads calculated according to ACI 440.1R-06 and Eurocode 2 are underestimated. This underestimation can be caused by the value of the ultimate concrete strain ε_{cu} which is assumed in these codes. It is lower than the value of ε_{cu} obtains in experiments.
- The nonlinear model of concrete, which was adopted in the study, reflects relatively well the behaviour of the actual concrete.

ACKNOWLEDGMENTS

The paper was presented at the 8th International Conference AMCM 2014 – Analytical Models and New Concepts in Concrete and Masonry Structures (AMCM'2014), Wrocław, June 2014.

REFERENCES

[1] Federation International du Beton, FRP reinforcement in RC structures, Fib Task, Group 9.3, 2007, pp.3-30

[2] ACI 440.1R-06, Guide for the design and construction of structural concrete reinforced with FRP bars, ACI Committee 440, 2006

[3] *Nanni A.*; North American design guidelines for concrete reinforcement and strengthening using FRP: Principals, applications and unresolved issues, Construction and Building Materials, Vol.17, No.6-7, 2003; p.439-446

[4] *Barris C., Torres L., Comas J., Mias C.*; Cracking and deflections in GFRP RC beams: an experimental study, Composites: Part B, Vol.55, 2013; p.580-590

[5] EN 1992-1-1:2003, Eurocode 2: Design of concrete structures – Prat 1-1: General rules and rules for buildings, Technical Committee CEN/TC250, 2004

[6] ABAQUS, Abaqus analysis user's manual, Version 6.10, Dassault Systemes, 2010

[7] *Lubliner J., Oliver J., Oller S., Onate E.*; A plastic-damage model for concrete, International Journal of Solids Mechanics, Vol.25, No.3, 1989; p.299-326

[8] *Lee J., Fenves G.L.*; Plastic-damage model for cyclic loading of concrete structures, Journal of Engineering Mechanics, Vol.124, No.8, 1998; p.892-900

[9] *Park R., Paulay T.*; Reinforced concrete structures, John Willey & Sons, 1975

[10] *Wang T., Hsu T.T.C.*; Nonlinear Finite Element Analysis of concrete structures using new constitutive models, Computers and Structures, Vol.79, No.32, 2001, p.2781-2791

[11] *Barris C., Torres L., Tauron A., Baena M., Catalan A.*; An experimental study of the flexural behaviour of GFRP RC beams and comparison with prediction-models, Composites Structures, Vol.91, 2009; p.586-295